PERGAMON

Engineering Fracture Mechanics 66 (2000) 15–39

Engineering Fracture Mechanics

www.elsevier.com/locate/engfracmech

Elastic–plastic analysis of off-center cracks in cylindrical structures

Robert Firmature[a], Sharif Rahman[b,*]

[a]*IBM Printing Systems Company, Boulder, CO 80301, USA*
[b]*Department of Mechanical Engineering, The University of Iowa, Iowa City, IA 52242, USA*

Received 1 July 1999; received in revised form 13 October 1999; accepted 19 November 1999

Abstract

This paper presents new elastic and elastic–plastic finite element solutions of the *J*-integral for a pipe containing off-center through-wall cracks under pure bending. The analysis is based on a three-dimensional nonlinear finite element method and small-strain theory. One hundred and five analyses were performed using the ABAQUS commercial code for a wide variety of crack sizes, off-center crack angles, and material hardening exponents. The results from these analyses show that the *J*-integral values at the two crack fronts of an off-center crack are unequal due to the loss of symmetry with respect to the bending plane of the pipe. In addition, the *J*-integral is larger, and hence, critical at the crack front which is farther away from the bending axis of the pipe. This is because, at that crack front, the tensile stress is larger and the component of the applied bending moment about the crack centerline has a further crack-opening effect. Also at this crack front, the *J* values can be lower or slightly higher than those of a symmetrically centered crack, depending on the crack size and off-centered angle. For the crack front that is closer to the bending axis, the *J* values are always lower than those of a symmetrically centered crack. This implies that the load-carrying capacity of a pipe is usually larger for an off-center crack than that for a symmetrically centered crack. Finally, based on these finite element solutions, new analytical expressions of *J*-integral were developed for fracture analysis of pipes containing off-center cracks.

Keywords: *J*-integral; Elastic–plastic fracture mechanics; Off-center crack; Pipe; Through-wall crack; Leak-before-break; *J*-estimation method

1. Introduction

Fracture analysis of pipes with circumferential cracks is an important task for leak-before-break

* Corresponding author. Tel.: +1-319-335-5679; fax: +1-319-335-5669.
E-mail address: rahman@icaen.uiowa.edu (S. Rahman).

0013-7944/00/$ - see front matter
PII: S0013-7944(99)00135-6

(LBB) [1,2] and pipe flaw evaluations [3]. Fig. 1 shows the cross-sectional geometry of three idealized circumferential cracks, which illustrate a simple through-wall crack (TWC), an internal surface crack, and a complex crack in a pipe. These cracks are frequently used to evaluate structural integrity and reliability of degraded piping systems. To evaluate its integrity under bending or combined bending and tension (pressure-induced) loads, the fracture response characteristics, such as crack-opening displacement and J-integral, are typically evaluated by assuming that these flaws are symmetrically placed with respect to the bending plane of the pipe (see Fig. 1). This is usually justified with the reasoning that the tensile stress due to bending is largest at the center of this symmetric crack. However, in real life, fabrication imperfections occur randomly around the pipe circumference. Additionally, during the normal operating condition of a power plant, the stress component due to pressure is far more significant than that due to bending. As such, the postulated flaw in LBB analysis may be off-centered and can thus be located anywhere around the pipe circumference. The likelihood of a crack being off-centered can be further emphasized in light of the argument that a symmetric bending plane under normal operating stress may become very different under normal and safe-shutdown earthquake stress, due to the uncertainty in the seismic ground motion [4–6].

Analytical and computational methods for fracture analysis of symmetrically–centered, circumferential, TWC pipes subjected to pure bending, pure tension, and combined bending and tension are well-developed. During the U.S. Nuclear Regulatory Commission's *Short Cracks in Piping and Piping Welds Program* [7], the currently available methods were evaluated by extensive comparisons with the experimental data. Two major technical reports, published by Brust et al. [8] and Rahman et al. [4], describe these methods and associated results involving various pipe geometries, crack sizes, and material properties. Although much has been learned about the behavior of symmetrically centered cracks, the current methods are incapable of predicting fracture response and crack growth behavior of off-center cracks, even though off-center cracks may be a concern of practical interest for both LBB and pipe flaw evaluations [9]. Hence, a fracture-mechanics study of off-center cracks is an exciting research area for improved evaluation of piping and pressure vessel integrity.

In the past, Rahman and coworkers investigated the crack-opening behavior of TWC pipes with both symmetrically centered [10–12] and off-center [5,6,12] cracks subject to pure bending loads. One of these studies developed a computational framework for analyzing off-center cracks based on the linear-elastic finite element method (FEM) [5,6]. Pipe-specific finite element calculations showed that the reduced crack-opening area (COA) for a pipe with an off-center crack can be determined by normal analysis procedures for a symmetrically centered crack via resolution of applied moment and assuming an elliptical crack-opening profile. This was an important finding for the leak-rate analysis part of LBB, since accuracy in the prediction of COA is more important than that of the entire crack-opening shape. Furthermore, the results indicated that due to reduced COA, a postulated crack size for LBB analysis will be larger (depending on the off-center angle) for the off-center cracks than that for the symmetrically centered cracks. However, it can also be argued that when a crack is off-centered, the crack-driving force, be it stress-intensity factor in linear-elastic fracture or J-integral in elastic–plastic fracture, will be lower than that for a symmetrically centered crack. Hence, an off-centered crack may increase the length of the postulated leaking flaw due to reduced crack-opening and cause a detrimental effect, but it can also have a beneficial effect on the maximum load-carrying capacity of pipes. In the previous work of Rahman et al. [5,6], only the crack-opening aspect of off-center cracks has been addressed. No methods have been developed or fracture analyses have been reported yet to predict crack-driving force and, hence, load-carrying capacity of pipes containing off-center cracks.

This paper presents new results from elastic and elastic–plastic fracture analyses of circumferential TWC pipes with off-center cracks subject to pure bending loads. The analyses are based on a three-dimensional nonlinear FEM and small-strain theory. The analyses were performed for a pipe with a radius-to-thickness ratio of 10 and a wide variety of crack size, off-center angles, and material hardening

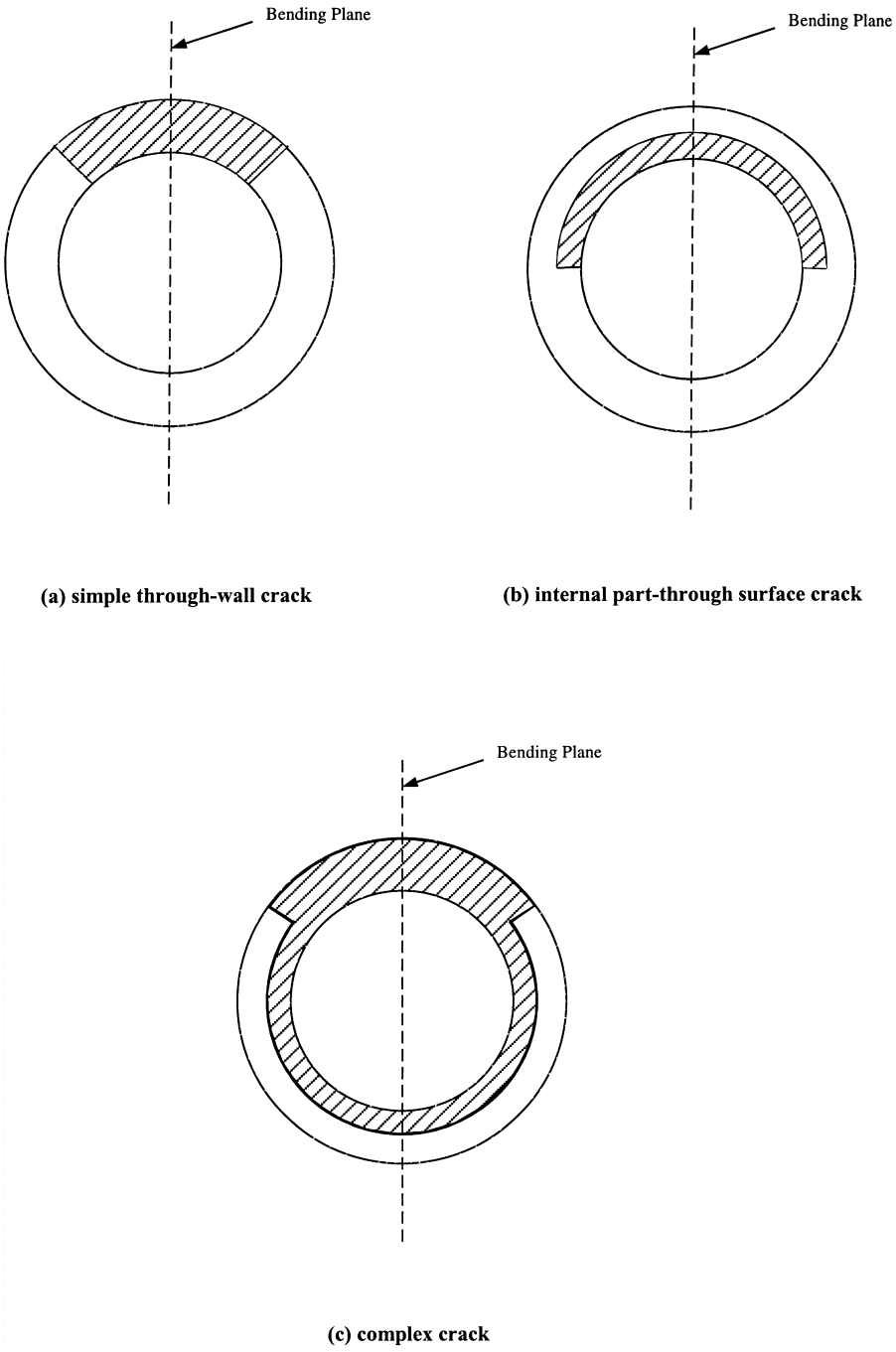

Fig. 1. Examples of symmetrically centered cracks in pipes: (a) simple through-wall crack, (b) internal part-through surface crack, and (c) complex crack.

characteristics. The finite element solutions were studied to evaluate the effects of off-centered cracks on the J-integral. Subsequently, these FEM results were used to develop new analytical expressions of influence functions for fracture analysis of pipes containing off-center cracks.

2. A TWC pipe with an off-center crack

Consider a TWC pipe with mean radius, R_m, wall thickness, t, and a TWC angle, 2θ. The crack is off-centered by an angle, ψ. The pipe is subjected to a pure bending moment, M, without any internal

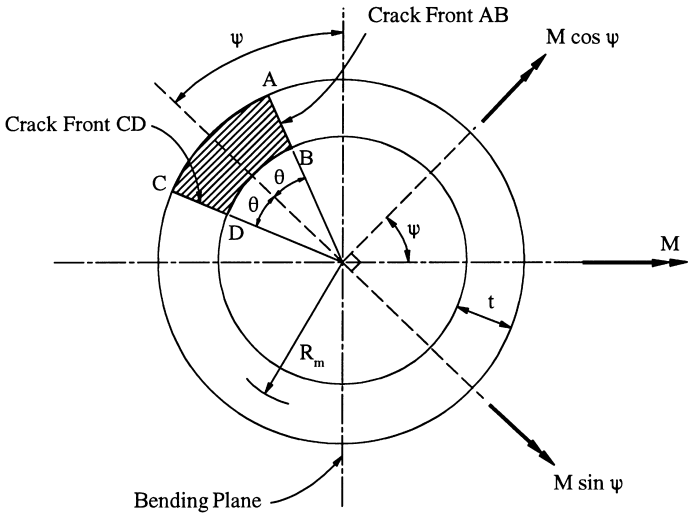

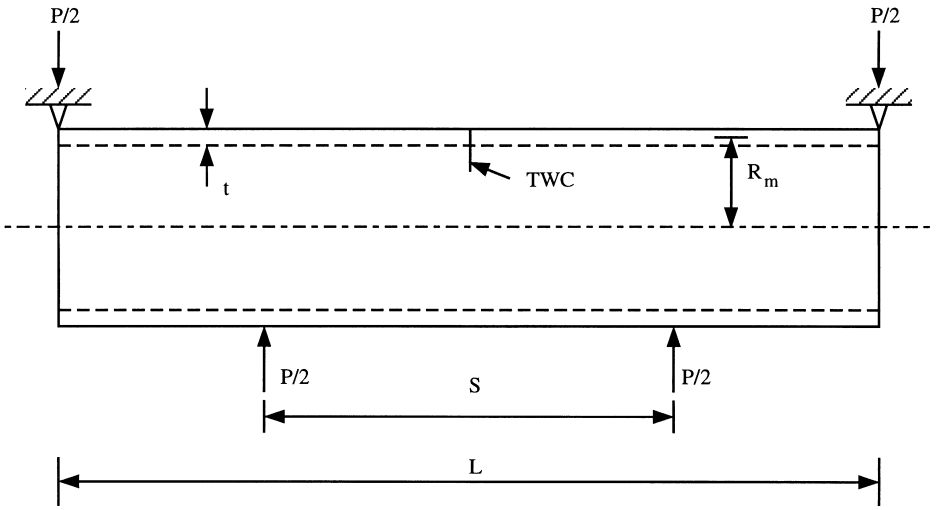

Fig. 2. An off-center through-wall crack in a pipe under pure bending.

pressure. This loading can be simulated by a four-point bend test as shown in Fig. 2. In this figure, S is the inner span, L is the outer span, and P is the total applied load. The geometric parameters of this off-center crack in the cracked section are also defined in Fig. 2.

In order to perform elastic–plastic analysis, the material model needs to be defined. In this study, it was assumed that the constitutive law characterizing the material's uniaxial stress–strain (σ–ε) response can be represented by the well-known Ramberg–Osgood model, which is

$$\frac{\varepsilon}{\varepsilon_0} = \frac{\sigma}{\sigma_0} + \alpha\left(\frac{\sigma}{\sigma_0}\right)^n \tag{1}$$

where σ_0 is the reference stress which can be arbitrary, but is usually assumed to be the yield stress, E is the modulus of elasticity, $\varepsilon_0 = \sigma_0/E$ is the associated reference strain, and α and n are the model parameters usually chosen from a best fit of actual laboratory data. Although this representation of the stress–strain curve is not necessary for the finite element analysis (FEA), it is needed for most J-estimation methods, which are formulated based on power-law idealization.

3. Elastic–plastic fracture mechanics

The J-integral fracture parameter proposed by Rice [13] has been extensively used in assessing fracture integrity of cracked engineering structures, which undergo large plastic deformation at the crack tip. For elastic–plastic problems, its interpretation as the strength of the asymptotic crack-tip fields by Hutchinson [14] and Rice and Rosengren [15] represents the crux of the basis for "J-controlled" crack growth behavior. For a cracked body with an arbitrary counter-clockwise path, Γ around the crack tip, a formal definition of J-integral under mode-I condition is

$$J \stackrel{\text{def}}{=} \int_{\Gamma} \left(\mathscr{W} n_1 - T_i u_{i,\,1}\right) \mathrm{d}\Gamma \tag{2}$$

where $\mathscr{W} = \int \sigma_{ij}\,\mathrm{d}\varepsilon_{ij}$ is the strain energy density with σ_{ij} and ε_{ij} representing components of stress and strain tensors, respectively, u_i and $T_i = \sigma_{ij} n_j$ are the ith components of displacement and traction vectors, n_j is the jth component of unit outward normal to integration path, $\mathrm{d}\Gamma$ is the differential length along contour Γ, and $u_{i,\,1} = \partial u_i/\partial x_1$ is the differentiation of displacement with respect to x_1. Here, the summation convention is adopted for repeated indices.

4. Finite element simulation

The FEM in this study assumed the elastic–plastic constitutive relation given by Eq. (1) and small strains. It was based on proportional loading in the crack-tip plastic zone. Hence, the use of deformation theory of plasticity and Eq. (1) is entirely appropriate. The plastic deformation was assumed to be incompressible and independent of hydrostatic stress, $\frac{1}{3}\sigma_{ii}$. An isotropic hardening rule was assumed. Under these conditions, the generalized multiaxial stress–strain relation becomes

$$\varepsilon_{ij} = \frac{1+\nu}{E} S_{ij} + \frac{1-2\nu}{3E}\sigma_{ll}\delta_{ij} + \frac{3}{2}\alpha\varepsilon_0\left(\frac{\sigma_{\mathrm{e}}}{\sigma_0}\right)^{n-1}\frac{S_{ij}}{\sigma_0} \tag{3}$$

where ν is Poisson's ratio, δ_{ij} is the Kronecker delta, $S_{ij} = \sigma_{ij} - \frac{1}{3}\sigma_{kk}\delta_{ij}$ is the deviatoric stress, and $\sigma_{\mathrm{e}}^2 = (\frac{3}{2}S_{ij}S_{ij})$ is the square of the *von Mises* equivalent stress. While the analysis is for small strains,

nonlinearity enters through Eq. (1) or Eq. (3). Note, Eq. (3) reduces to Eq. (1) for a uniaxial state of stress.

4.1. Finite element implementation of J

For numerical calculation of J, the energy domain integral methodology [16,17] was used in the FEA. This methodology is versatile, as it can be applied to both quasi-static and dynamic fracture problems with elastic, plastic, or viscoplastic material response, as well as thermal loading. In addition, the domain integral formulation is relatively simple to implement numerically in a finite element code.

Using the divergence theorem, the contour integral defined in Eq. (2) can be expanded into a volume integral in three-dimensions over a finite domain surrounding the crack tip or crack front. For a linear or nonlinear elastic material under a quasi-static condition, in the absence of body forces, thermal strains, and crack-face tractions, Eq. (2) for a three-dimensional pipe problem reduces to

$$J = \int_{V^*} \left(\sigma_{ij} \frac{\partial u_j}{\partial x_1} - \mathscr{W} \delta_{1i} \right) \frac{\partial q}{\partial x_i} \, \mathrm{d}V \tag{4}$$

where q is an arbitrary but smooth weighting function and V^* is the volume enclosed by the inner surface S_0 and outer surface S_1 as shown in Fig. 3. The discrete form of this domain integral is [18]

$$J \cong \sum_{V^*} \sum_{l=1}^{m} \left\{ \left[\left(\sigma_{ij} \frac{\partial u_j}{\partial x_1} - \mathscr{W} \delta_{1i} \right) \frac{\partial q}{\partial x_i} \right] \frac{\partial x_j}{\partial \xi_k} \right\}_l w_l \tag{5}$$

where m is the number of Gauss points per element, ξ_k is the parametric coordinate, and w_l is the weighting factor. Further details on finite element implementation of J are given by Anderson [18].

The domain integral method described above is implemented into the ABAQUS commercial finite element code (Version 5.6) [19]. The method is quite robust in the sense that accurate estimates of the J-integral are usually obtained even with coarse meshes. This is because the integral is evaluated over a

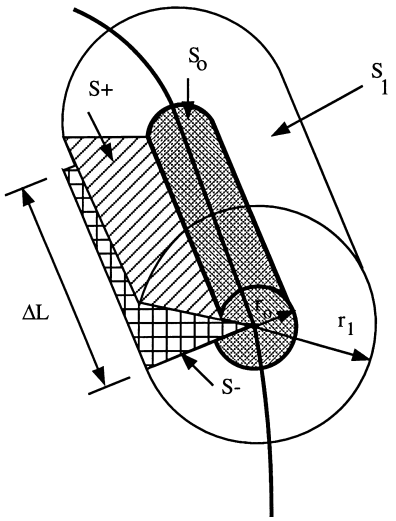

Fig. 3. Inner and outer surfaces enclosing V^*.

domain of elements surrounding the crack front, so that the errors in local solution parameters have a lesser effect on the calculated value.

4.2. Matrix of analysis and finite element models

For calculating the J-integral for off-center cracks, 105 elastic–plastic FEAs were conducted for the pipe in Fig. 2 with $R_m = 50.8$ mm (2 in.) and $t = 5.08$ mm (0.2 in.). A matrix of such analyses is defined in Table 1 for various combinations of the crack size, crack orientation, and material strain hardening exponent: θ/π, ψ, and n. It involves 21 different finite element meshes with $\theta/\pi = 1/16$, 1/8, and 1/4 and $\psi = 0$, 15, 30, 45, 60, 75, and 90°. In this paper, a crack will be denoted as small, intermediate, and large, when $\theta/\pi = 1/16$, 1/8, and 1/4, respectively. For each mesh, five analyses were performed using five different hardening exponents (see Table 1). For the material properties, the following values were used: $E = 207$ GPa, $\nu = 0.3$, $\sigma_0 = 344.8$ MPa, and $\alpha = 0$ for $n = 1$ and $\alpha = 1$ for $n > 1$. These values, in addition to the ones given in Table 1, provide complete characterization of the pipe material properties according to Eqs. (1) and (3).

Fig. 4(a) and (b) show two finite element meshes for pipes with a symmetrically centered crack and an off-centered crack ($\psi = 45°$), respectively. These meshes were developed for a small crack ($\theta/\pi = 1/16$) using the MSC/PATRAN (Version 7.0) solid modeler [20]. Since the symmetry is broken with respect to the crack geometry (except when $\psi = 0$), these meshes involved a half model to take advantage of the remaining symmetry with respect to the crack plane. Twenty-noded isoparametric solid elements were used with focused elements at the crack tip. Fig. 5 shows the amplified view of the mesh illustrating these focused elements. In the crack-tip region, a ring of 12 wedge-shaped elements was used. These

Table 1
Matrix of finite element analyses for off-center cracks (five runs per model)

FEM model no.	θ/π	ψ (deg)[a]	n[b]
1	1/16	0	1, 3, 5, 7, and 10
2	1/16	15	1, 3, 5, 7, and 10
3	1/16	30	1, 3, 5, 7, and 10
4	1/16	45	1, 3, 5, 7, and 10
5	1/16	60	1, 3, 5, 7, and 10
6	1/16	75	1, 3, 5, 7, and 10
7	1/16	90	1, 3, 5, 7, and 10
8	1/8	0	1, 3, 5, 7, and 10
9	1/8	15	1, 3, 5, 7, and 10
10	1/8	30	1, 3, 5, 7, and 10
11	1/8	45	1, 3, 5, 7, and 10
12	1/8	60	1, 3, 5, 7, and 10
13	1/8	75	1, 3, 5, 7, and 10
14	1/8	90	1, 3, 5, 7, and 10
15	1/4	0	1, 3, 5, 7, and 10
16	1/4	15	1, 3, 5, 7, and 10
17	1/4	30	1, 3, 5, 7, and 10
18	1/4	45	1, 3, 5, 7, and 10
19	1/4	60	1, 3, 5, 7, and 10
20	1/4	75	1, 3, 5, 7, and 10
21	1/4	90	1, 3, 5, 7, and 10

[a] $\psi = 0$ implies symmetrically centered crack.
[b] $n = 1$ implies linear-elastic analysis when $\alpha = 0$ (see Eq. (1) or Eq. (3)).

wedge-shaped elements were constructed by collapsing the appropriate nodes of 20-noded solid elements to produce a $1/r$ strain singularity. Although this singularity is strictly valid for a fully plastic crack-tip field in a non-hardening material ($n \to \infty$), it is in practice adequate for work-hardening materials with a sufficiently refined crack-tip mesh [21–29]. In the finite element meshes shown in Fig. 4 or Fig. 5, the smallest crack-tip element size in the circumferential direction is about 8% of the crack length.

Each FEA was performed in a single load step, which consisted of increasing the bending load, $P/2$ (see Fig. 2) in 10 increments. In all analyses, the algorithm of deformation theory of plasticity was used. A reduced $2 \times 2 \times 2$ Gaussian quadrature rule was used for the numerical integration. All analyses were performed using the commercial finite element code ABAQUS [19].

4.3. Verification with existing solutions

First, a selected number of FEAs were performed to validate the results of the J-integral of TWC pipes by comparing with existing solutions in the literature. Since there are no data or results available for off-center cracks, this validation was limited to symmetrically centered cracks in pipes only. Both elastic and elastic–plastic analyses were performed.

Fig. 6 shows the plots of J-integral of a symmetrically centered crack in a TWC pipe as a function of applied bending moment for "small" ($\theta/\pi = 1/16$), "intermediate" ($\theta/\pi = 1/8$), and "large" ($\theta/\pi = 1/4$) cracks. The results were obtained from elastic ($\alpha = 0, n = 1$) analysis of a pipe under pure bending load. In Fig. 6, the plots involve three sets of results — one is from the present FEA, and the other two are

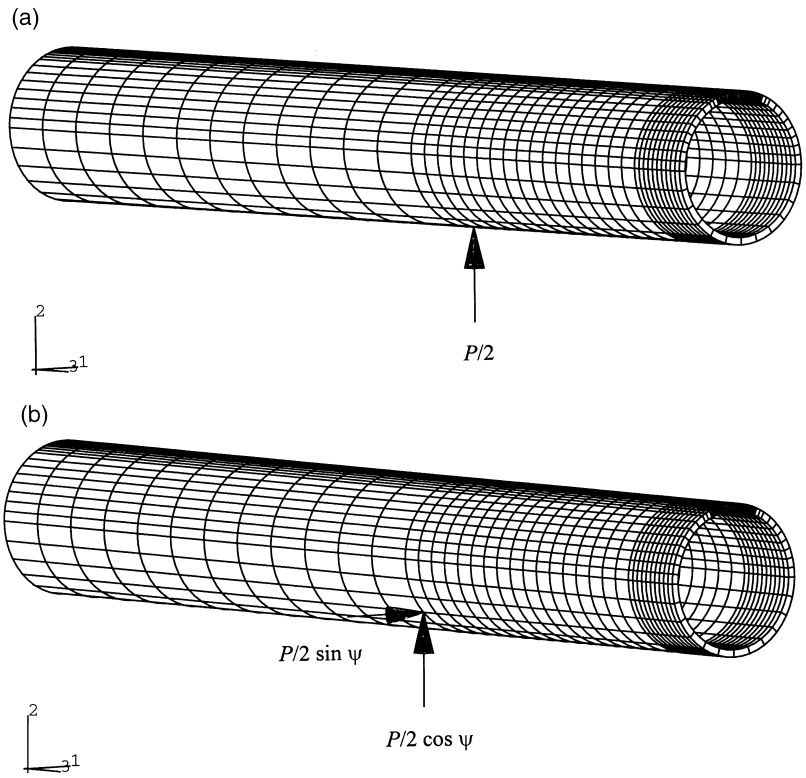

Fig. 4. Finite element meshes for symmetrically centered and off-centered cracks in pipes: (a) a symmetrically centered crack ($\theta/\pi = 1/16, \psi = 0^\circ$) and (b) an off-centered crack ($\theta/\pi = 1/16, \psi = 45^\circ$).

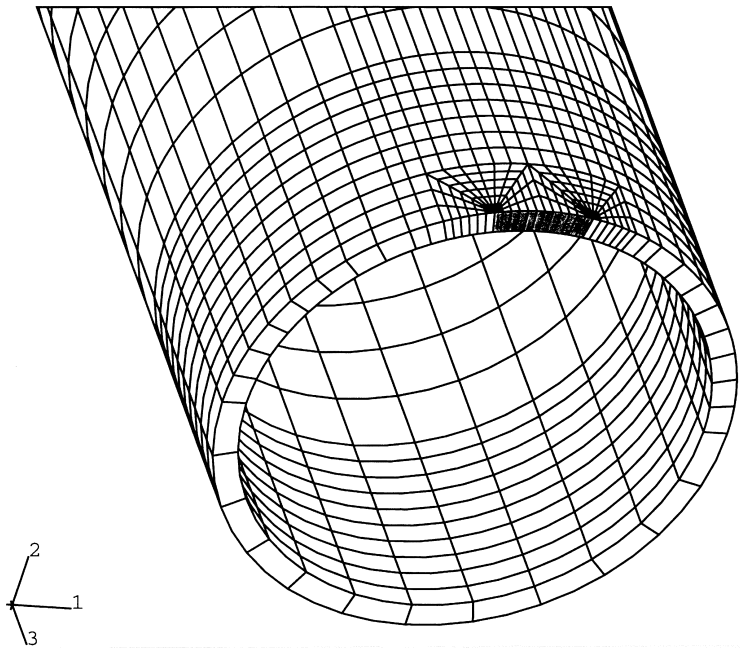

Fig. 5. Crack-tip mesh refinement ($\theta/\pi = 1/16$).

based on the well-known GE/EPRI J-estimation formula using the elastic influence functions of Kumar et al. [30,31] and Brust et al. [32,33].[1] The analyses were continued until M was considerably larger than the reference moment, M_0, of the pipe, defined by Kumar et al. [30,31].[2] As seen in Fig. 6, the three sets of results are in close agreement with each other for all crack sizes considered in this study.

In addition to this elastic validation of J, similar comparisons were also made for an elastic–plastic case with a specific value of $n = 5$. As before, the analyses were conducted for three crack sizes with $\theta/\pi = 1/16$, 1/8, and 1/4. The comparisons of results from this study with the GE/EPRI solutions are presented in Fig. 7. The elastic–plastic FEM results match very well with the existing solutions. This verification gave confidence in our finite element calculations.

4.4. Results and discussions

According to Table 1, 21 finite element meshes similar to the ones in Fig. 4 or Fig. 5, were developed [35,36]. For each mesh, five analyses were performed for $n = 1$, 3, 5, 7, and 10. For brevity, only the results of the elastic analysis ($n = 1$) and elastic–plastic ($n = 5$) analysis will be discussed in this paper. Detailed results are available in Ref. [35].

4.4.1. Elastic analysis

Fig. 8(a) and (b) show the results of J vs. M plots from purely elastic ($n = 1$) analyses of small cracks

[1] In both studies by Kumar et al. [30,31] and Brust et al. [32,33], the influence functions defined by the GE/EPRI method were derived from FEAs. The analysis by Kumar et al. involved the ADINA code [34] using nine-noded shell elements. The analysis by Brust et al. involved the ABAQUS code [19] using 20-noded solid elements.

[2] According to the GE/EPRI J-estimation formula given by Kumar et al. [30,31], $M_0 = 4\sigma_0 R_m^2 t(\cos\frac{\theta}{2} - \frac{1}{2}\sin\theta)$.

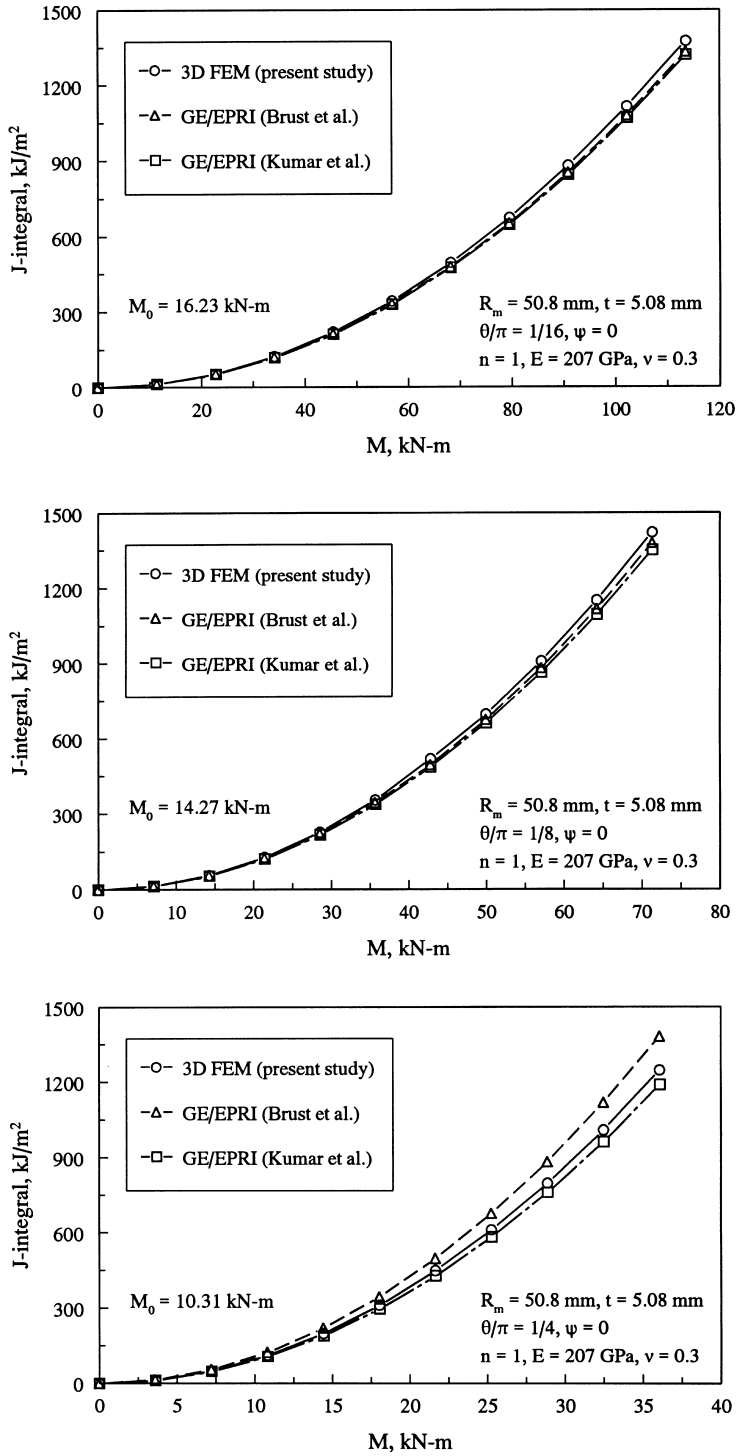

Fig. 6. Comparisons of predicted J from elastic analysis of symmetric cracks with existing solutions.

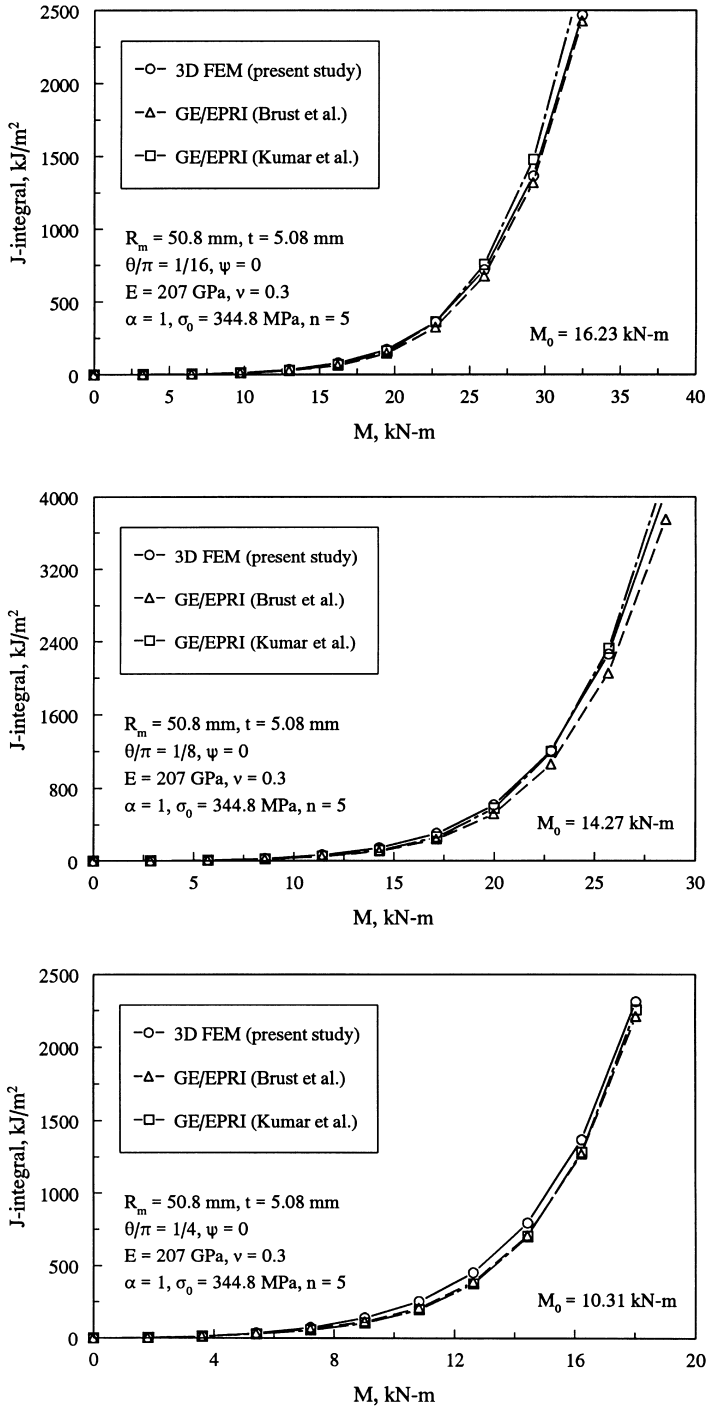

Fig. 7. Comparisons of predicted J from elastic–plastic analysis of symmetric cracks with existing solutions.

($\theta/\pi = 1/16$) for the two crack fronts AB and CD (see Fig. 2), respectively. The analyses involved various off-center crack angles with $\psi = 0$, 15, 30, 45, 60, 75, and 90°. The results in Fig. 8(a) and (b) represent the average values of J over the wall thickness. They indicate that the J-integral for a symmetrically centered crack is larger than that for an off-centered crack. This is due to the fact that the tensile stress due to bending is largest at the center of a symmetric crack. Except for $\psi = 0$, which represents a symmetrically centered crack, Fig. 8(a) and (b) also show that the J values for off-center cracks are larger at crack front AB than at crack front CD. This is because: (1) the tensile stress at crack front AB is larger than that at crack front CD and (2) the moment component, $M \sin\psi$, has a crack-opening effect on crack front AB, while it has a crack-closing effect on crack front CD.

Fig. 9 and Fig. 10 show similar results of J for the intermediate ($\theta/\pi = 1/8$) and large ($\theta/\pi = 1/4$) crack sizes, respectively. With the exception of the 15° offset angle, the intermediate and large crack

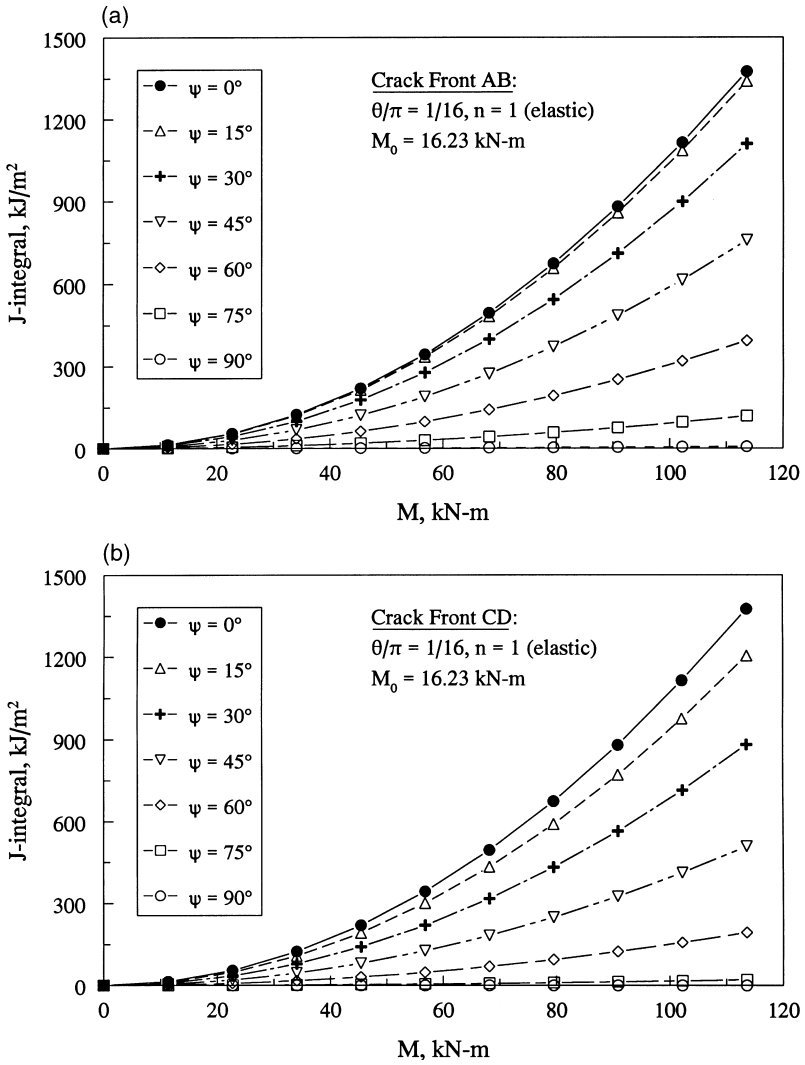

Fig. 8. J-integral vs. bending moment from elastic analysis of a small crack ($\theta/\pi = 1/16$): (a) crack front AB and (b) crack front CD.

sizes display a behavior similar to the small crack. For these larger cracks with a small offset, it was observed that the J values were actually slightly higher than those for the centered crack case at crack front AB. This can be explained by noting that for an incremental increase in the offset angle from the centered position, crack front AB will be placed into a higher stress region which can lead to the increased J values as observed in this study. Extending this argument even further, it is postulated that for any crack size, there will exist a threshold of offset angle below which the J values at crack front AB exceed those of the centered crack. Unfortunately, this trend was not captured for the smaller cracks in this study due to the fact that for computational efficiency, the mesh was only designed for a 15°

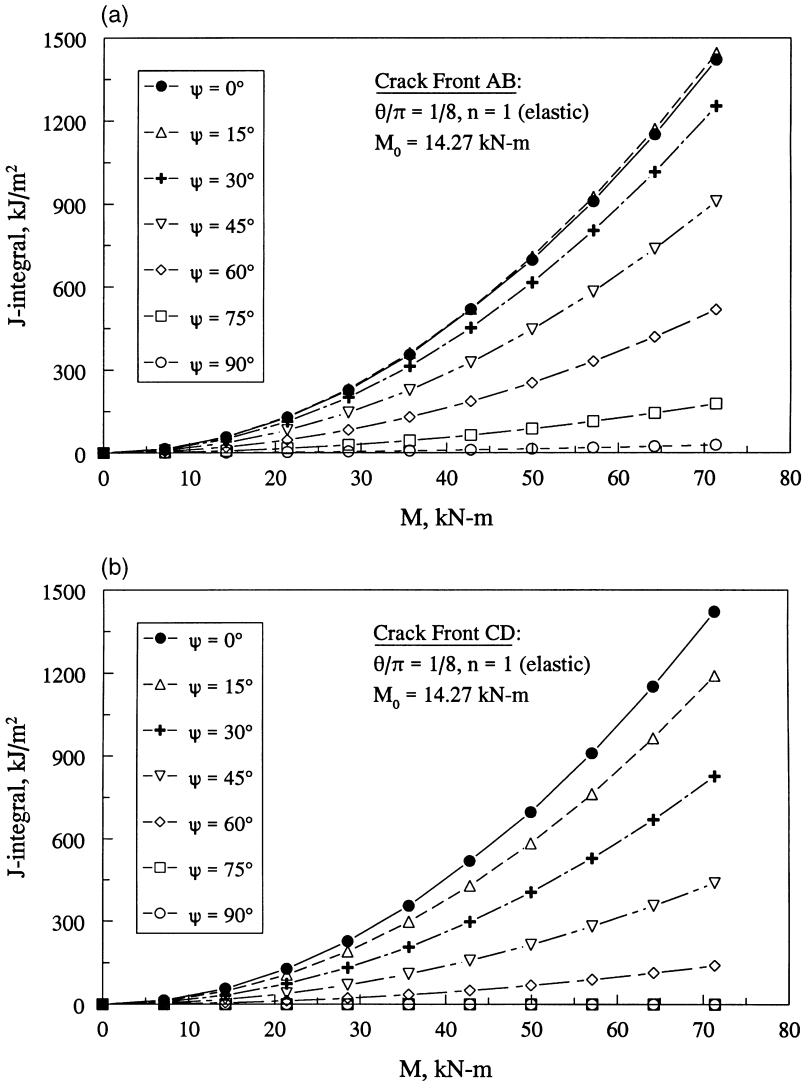

(b) crack front CD

Fig. 9. J-integral vs. bending moment from elastic analysis of a medium crack ($\theta/\pi = 1/8$): (a) crack front AB and (b) crack front CD.

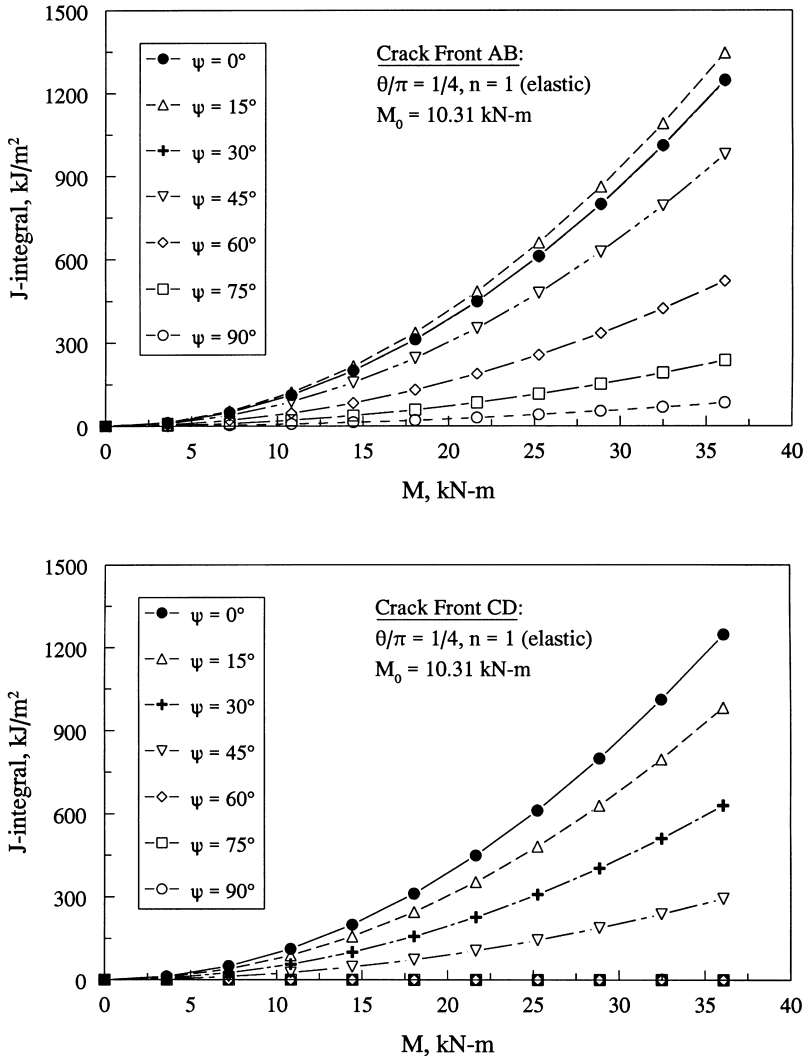

Fig. 10. *J*-integral vs. bending moment from elastic analysis of a large crack ($\theta/\pi = 1/4$): (a) crack front AB and (b) crack front CD.

increment of the offset angle. This threshold offset angle will increase as the crack size increases. Further investigations should be undertaken to determine this threshold of offset angle.[3]

4.4.2. Elastic–plastic analysis

Elastic–plastic analyses were also performed for a specific case of $n = 5$ to investigate the fracture behavior of off-center cracks in the presence of crack-tip plasticity. The results of these analyses are shown in Figs. 11, 12 and 13 in terms of J vs. M plots for small, intermediate, and large cracks, respectively. As before, the J-integral values are presented for both crack fronts AB and CD and various

[3] Upon further investigation, this particular offset angle threshold was less than 15° for $\theta/\pi = 1/16$.

off-center crack angles. The results suggest that due to plastic deformation, the J-integral values from elastic–plastic analysis are much higher than those from purely elastic analysis for a given applied moment. Otherwise, the trends in the elastic–plastic behavior of off-center cracks are very similar to those from purely elastic analysis.

The finite element results developed in this study, some of which are presented here, should be useful in quantifying the J-integral of off-center cracks in pipes, so that their load-carrying capacity can be predicted. In most cases, the J values for off-center cracks are smaller than those for symmetric cracks, except when the off-center angle is small. In the case of small off-center angles, the J-integral for off-center cracks at one crack front can be higher than that for symmetric cracks, but their difference is also small. When the off-center angle is large, the J values for off-center cracks can be reduced significantly, resulting in increased load-carrying capacity of pipes. It would be interesting to see how this increase in

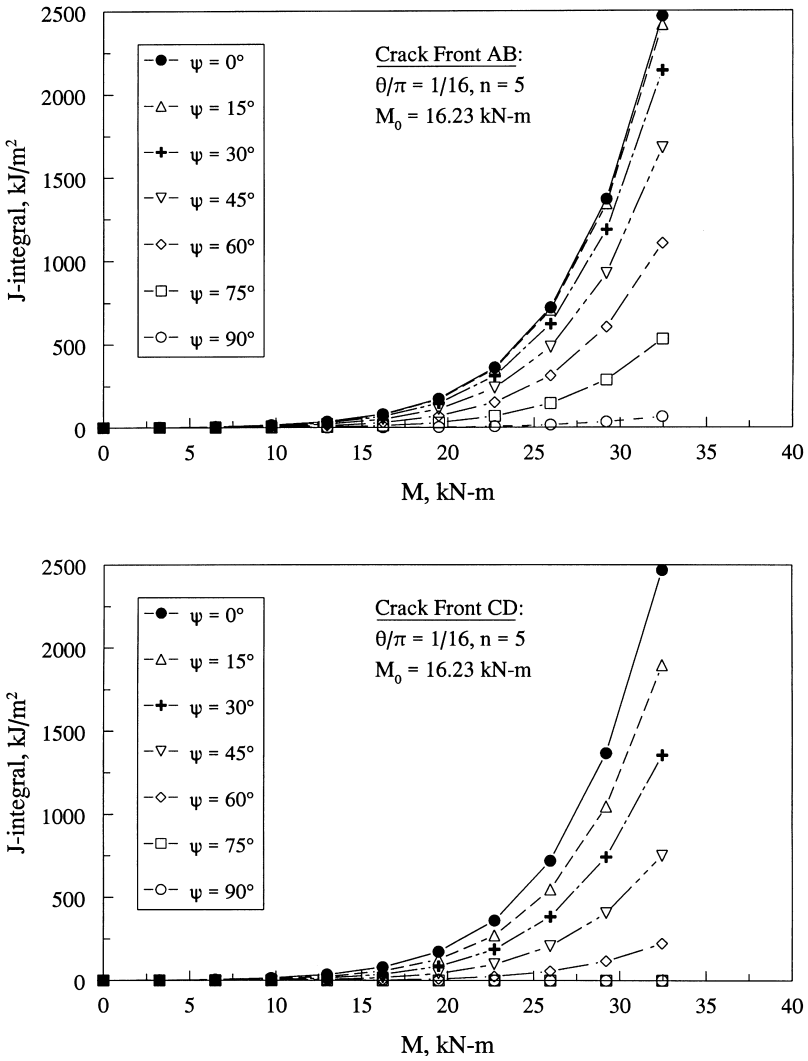

Fig. 11. J-integral vs. bending moment from elastic–plastic analysis of a small crack ($\theta/\pi = 1/16$): (a) crack front AB and (b) crack front CD.

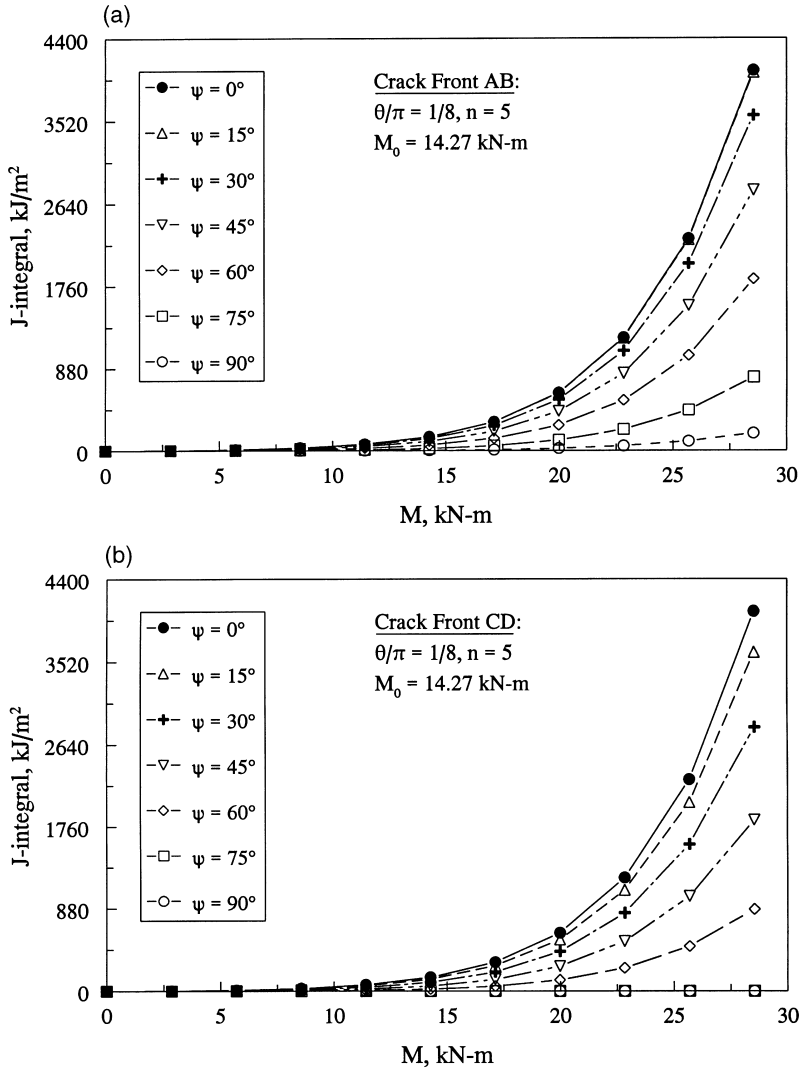

Fig. 12. J-integral vs. bending moment from elastic–plastic analysis of a medium crack ($\theta/\pi = 1/8$): (a) crack front AB and (b) crack front CD.

load-carrying capacity counters the reduced crack-opening for LBB applications. These FEM results can be used to develop analytical expressions of influence functions and J-integral for fracture analysis of pipes containing off-center cracks. These analytical expressions will allow both deterministic and probabilistic pipe fracture evaluations without any need to perform a full-scale nonlinear FEA. They are described in the next section.

5. A new J-estimation method

Under elastic–plastic conditions and applying the deformation theory of plasticity when the stress–strain curve is modeled by Eq. (1), the total crack driving force, J, for an off-centered crack of angle ψ

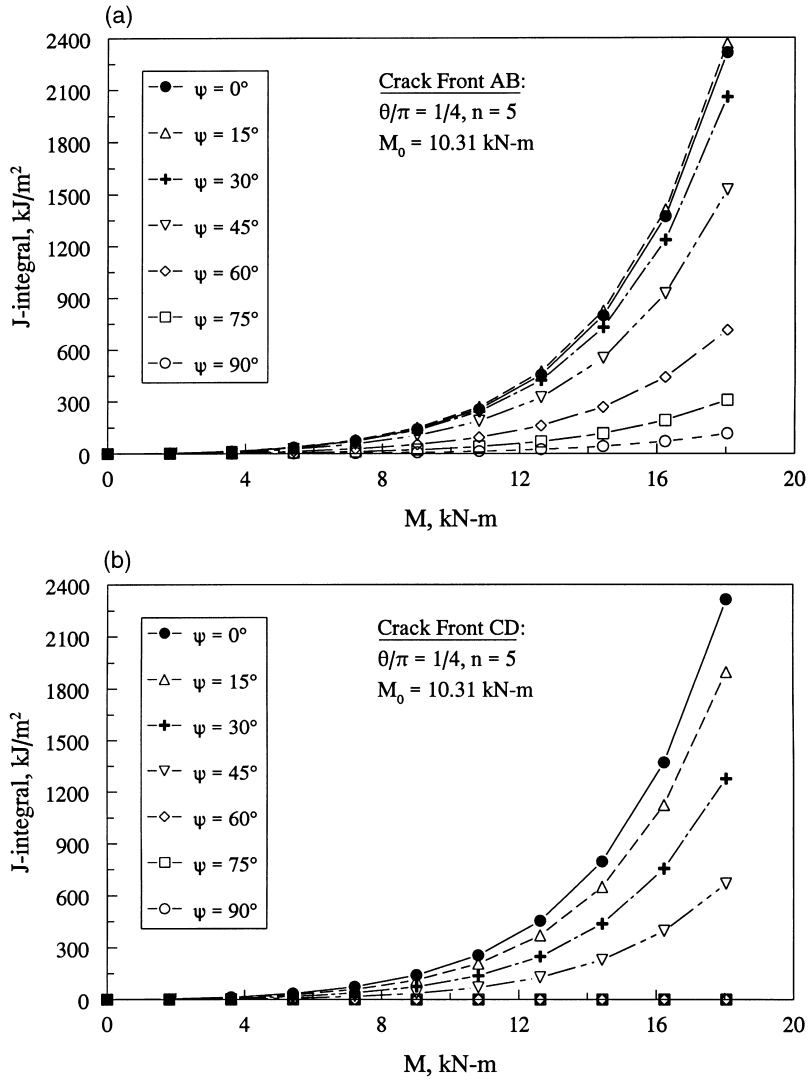

Fig. 13. *J*-integral vs. bending moment from elastic–plastic analysis of a large crack ($\theta/\pi = 1/4$): crack front AB and (b) crack front CD.

can be obtained by adding the elastic component, $J_{e,\psi}$, and the plastic component, $J_{p,\psi}$, i.e.,

$$J = J_{e,\psi} + J_{p,\psi}. \tag{6}$$

Closed-form equations already exist for the elastic and plastic components of a symmetrically centered crack [30–33]. It is proposed to use these equations along with simple off-center-angle correction factors for the calculation of $J_{e,\psi}$ and $J_{p,\psi}$. Hence, Eq. (6) can be re-written as

$$J = J_{e,0}K_{e,\psi} + J_{p,0}K_{p,\psi} \tag{7}$$

where

$$J_{e,0} = \frac{\theta}{\pi} F(\theta/\pi, R_m/t)^2 \frac{M^2}{E R_m^3 t^2} \tag{8}$$

and

$$J_{p,0} = \frac{\alpha \sigma_0^2}{E} R_m \theta \left(1 - \frac{\theta}{\pi}\right) h_1(\theta/\pi, n, R_m/t) \left(\frac{M}{M_0}\right)^{n+1} \tag{9}$$

are the well-known GE/EPRI equations[4] [30–33] for elastic and plastic components of J, respectively, for a symmetrically centered crack, i.e., when $\psi = 0$, $F(\theta/\pi, R_m/t)$ and $h_1(\theta/\pi, n, R_m/t)$ are elastic and plastic influence functions for symmetrically centered cracks, M_0 is a reference moment, and $K_{e,\psi}$ and $K_{p,\psi}$ are constant elastic and plastic correction factors for off-center cracks, respectively. Note, an effective crack length using plastic-zone-size correction was used in the original GE/EPRI equations [30]. In this study, the actual crack length was used in Eqs. (6)–(9) since the plastic component of the J-integral is explicitly accounted for in Eq. (6). See Ref. [4,8] for justification of using actual crack length over effective crack length. The evaluations of $F(\theta/\pi, R_m/t)$ and $h_1(\theta/\pi, n, R_m/t)$ are described in Appendix A.

By comparing Eqs. (6) and (7), it is easy to show that

$$K_{e,\psi} = \frac{J_{e,\psi}}{J_{e,0}} \tag{10}$$

$$K_{p,\psi} = \frac{J_{p,\psi}}{J_{p,0}}. \tag{11}$$

With this new proposed method, i.e., Eq. (7), the J-integral for off-center cracks can be easily calculated when these two correction factors are prescribed for a given off-center angle, ψ.

5.1. Calculation of correction factors

From Eqs. (10) and (11), it can be seen that the proposed correction factors are simply a ratio of the J values for the off-centered crack to those of the symmetrically centered crack. Based on these equations and FEM solutions described in the previous sections, Table 2 shows the results of $K_{e,\psi}$ and $K_{p,\psi}$ at cracks fronts AB and CD for a pipe with $R_m/t = 10$ and various combinations of θ/π, ψ, and n. For an off-center angle of 0, the correction factors should have a value of 1, as is shown in Table 2. For the intermediate ($\theta/\pi = 1/8$) and large ($\theta/\pi = 1/4$) cracks, it is shown that at the 15° offset the correction factor values are sometimes greater than unity for crack front AB. This agrees with the trend discussed earlier in which J values at crack front AB with small offset angle are larger than the values obtained for a symmetrically centered crack. For all other cases, the correction factors are less than 1 reflecting the fact that most of the time the symmetrically centered crack is more critical than the off-centered crack. Correction factors close to 0 were also found for offset angles that move the crack front CD below the bending axis and, therefore, may cause it to be closed.

[4] Note, the well-known GE/EPRI method, which constitutes Eqs. (8) and (9), is one of the many J-estimation methods currently available for analyzing pipes with symmetrically centered cracks. See Refs. [4,8] for other J-estimation methods.

5.2. Response surface approximation of correction factors

In order to eliminate the interpolation that is usually necessary when using tabulated data, it was decided to fit the correction factors listed in Table 2 with an analytical equation. The data in Table 2 show almost linear variation with respect to the crack length, but their variation with respect to the offset angle is slightly more complex. Accordingly, a response surface equation given by

Table 2
Elastic and plastic correction factors for $R_m/t = 10$[a]

n	$\psi = 0^\circ$ (0 rad)	$\psi = 15^\circ$ ($\pi/12$ rad)	$\psi = 30^\circ$ ($\pi/6$ rad)	$\psi = 45^\circ$ ($\pi/4$ rad)	$\psi = 60^\circ$ ($\pi/3$ rad)	$\psi = 75^\circ$ ($5\pi/12$ rad)	$\psi = 90^\circ$ ($\pi/2$ rad)
				(a) Crack front AB ($\theta/\pi = 1/16$)			
1	1	0.974	0.807	0.552	0.287	0.087	0.004
3	1	0.979	0.862	0.668	0.430	0.196	0.021
5	1	0.980	0.870	0.685	0.455	0.222	0.027
7	1	0.980	0.872	0.688	0.458	0.229	0.03
10	1	0.980	0.867	0.677	0.447	0.224	0.03
				(b) Crack front AB ($\theta/\pi = 1/8$)			
1	1	1.016	0.882	0.640	0.364	0.125	0.020
3	1	1.002	0.898	0.708	0.472	0.203	0.047
5	1	0.993	0.882	0.689	0.458	0.198	0.048
7	1	0.984	0.858	0.654	0.424	0.179	0.042
10	1	0.973	0.821	0.596	0.366	0.145	0.032
				(c) Crack front AB ($\theta/\pi = 1/4$)			
1	1	1.079	0.998	0.784	0.418	0.190	0.068
3	1	1.033	0.930	0.729	0.374	0.173	0.070
5	1	1.014	0.872	0.639	0.291	0.124	0.048
7	1	0.994	0.805	0.537	0.206	0.080	0.029
10	1	0.970	0.724	0.431	0.138	0.048	0.016
				(d) Crack front CD ($\theta/\pi = 1/16$)			
1	1	0.875	0.641	0.370	0.141	0.015	–
3	1	0.920	0.752	0.525	0.278	0.071	–
5	1	0.929	0.775	0.557	0.312	0.094	–
7	1	0.934	0.783	0.568	0.323	0.108	–
10	1	0.936	0.783	0.564	0.322	0.117	–
				(e) Crack front CD ($\theta/\pi = 1/8$)			
1	1	0.837	0.581	0.309	0.099	–	–
3	1	0.892	0.695	0.449	0.207	–	–
5	1	0.896	0.703	0.460	0.222	–	–
7	1	0.892	0.691	0.445	0.215	–	–
10	1	0.880	0.661	0.407	0.197	–	–
				(f) Crack front CD ($\theta/\pi = 1/4$)			
1	1	0.787	0.505	0.236	–	–	–
3	1	0.833	0.582	0.322	–	–	–
5	1	0.825	0.559	0.298	–	–	–
7	1	0.812	0.520	0.258	–	–	–
10	1	0.791	0.474	0.216	–	–	–

[a] $\psi = 0$ implies symmetrically centered crack; $n = 1$ implies linear-elastic analysis ($\alpha = 0$); – crack front closed.

$$K_{I,\psi} = 1 + \left[a_0(n) + a_1(n)\left(\frac{\theta}{\pi}\right)\right]\psi + \left[a_2(n) + a_3(n)\left(\frac{\theta}{\pi}\right)\right]\psi^2 + \left[a_4(n) + a_5(n)\left(\frac{\theta}{\pi}\right)\right]\psi^3 + \left[a_6(n) + a_7(n)\left(\frac{\theta}{\pi}\right)\right]\psi^4$$

is proposed, where $K_{I,\psi}$ is either $K_{e,\psi}$ or $K_{p,\psi}$ (i.e., the elastic or plastic correction factor for an off-centered crack), and $a_i(n)$, $i = 0, 1, \ldots, 7$, are surface fit coefficients that depend on the material hardening parameter, n, for a pipe with a given R_m/t. The coefficients, $a_i(n)$, can be further approximated by a fourth-order polynomial equation represented by

$$a_i(n) = \sum_{j=0}^{4} D_{ij} n^j \tag{13}$$

in which D_{ij} ($i = 0, 1, \ldots, 7$ and $j = 0, 1, \ldots, 4$) are the polynomial coefficients that solely depend on the R_m/t ratio of the pipe. Following least-squares curve-fit of data in Table 2, D_{ij} were estimated and are given in Appendix B for a pipe with $R_m/t = 10$. Using these values of D_{ij}, Fig. 14(a) and (b) show the plots of $K_{e,\psi}$ ($n = 1$) and $K_{p,\psi}$ ($n = 5$), respectively, as a function of θ/π and ψ for a pipe with $R_m/t = 10$. From these plots, it appears that Eqs. (12) and (13) can accurately represent the data in Table 2. In fact, the square of correlation coefficient (R-squared statistic) between the surface fit equations and the finite element data was at least 99% for all cases considered in this study.

Note, the analytical approximation of $K_{I,\psi}$, represented by Eqs. (12) and (13), allows closed-from evaluation of J-integral for off-center cracks. This would significantly reduce the computational effort in performing any future probabilistic and crack-growth studies [37,38].

5.3. Limitations of response surface approximation

Even with a very good agreement between the calculated correction factors and their surface fits, two very important limitations still exist. First, because the finite element meshes were only designed for 15° increments, it is unknown how well the surface fits actually describe the behavior of crack front AB for offset angles lower than 15°. It was found that a threshold offset angle would exist below 15° for each of the three crack lengths in this research; however, these threshold values were not determined in this study. It is expected that a small error will exist in this region due to lack of data. For these reasons, it is recommended that the surface fit equations for crack front AB only be used for offset angles ranging from 15 to 90° and only for crack lengths between 1/16 and 1/4 of the pipe circumference.

The second limitation is also related to the 15° increment of the offset angle. Due to the set increment values and the varying crack lengths, the final data point for the two smaller cracks correspond to offset angles well before closure of crack front CD. Because of this, the behavior of crack front CD is unknown from the last data point until closure for the two smaller cracks. However, for $\theta/\pi = 1/4$, the final data point may fall at the largest offset for which front CD is not closed and, hence, a discontinuity may occur at this point. Hence, the smaller cracks are expected to behave similarly in the same configuration. Due to this fact, the surface fit equations for crack front CD give reasonable approximations up to crack closure since they show the correct trend of a discontinuity at crack closure. However, since there are no data for the two smaller cracks at the point of crack closure, a region of extrapolation is needed between the final nonzero data points and the closure line [35]. The crack closure line is simply a straight line defining one edge of the extrapolation region in the θ/π–ψ plane. The crack is closed when $\psi + \theta > 90°$. If crack front CD is closed, then a value of zero should be used for the correction factor. Otherwise, correction factor data in this area should be used with caution since

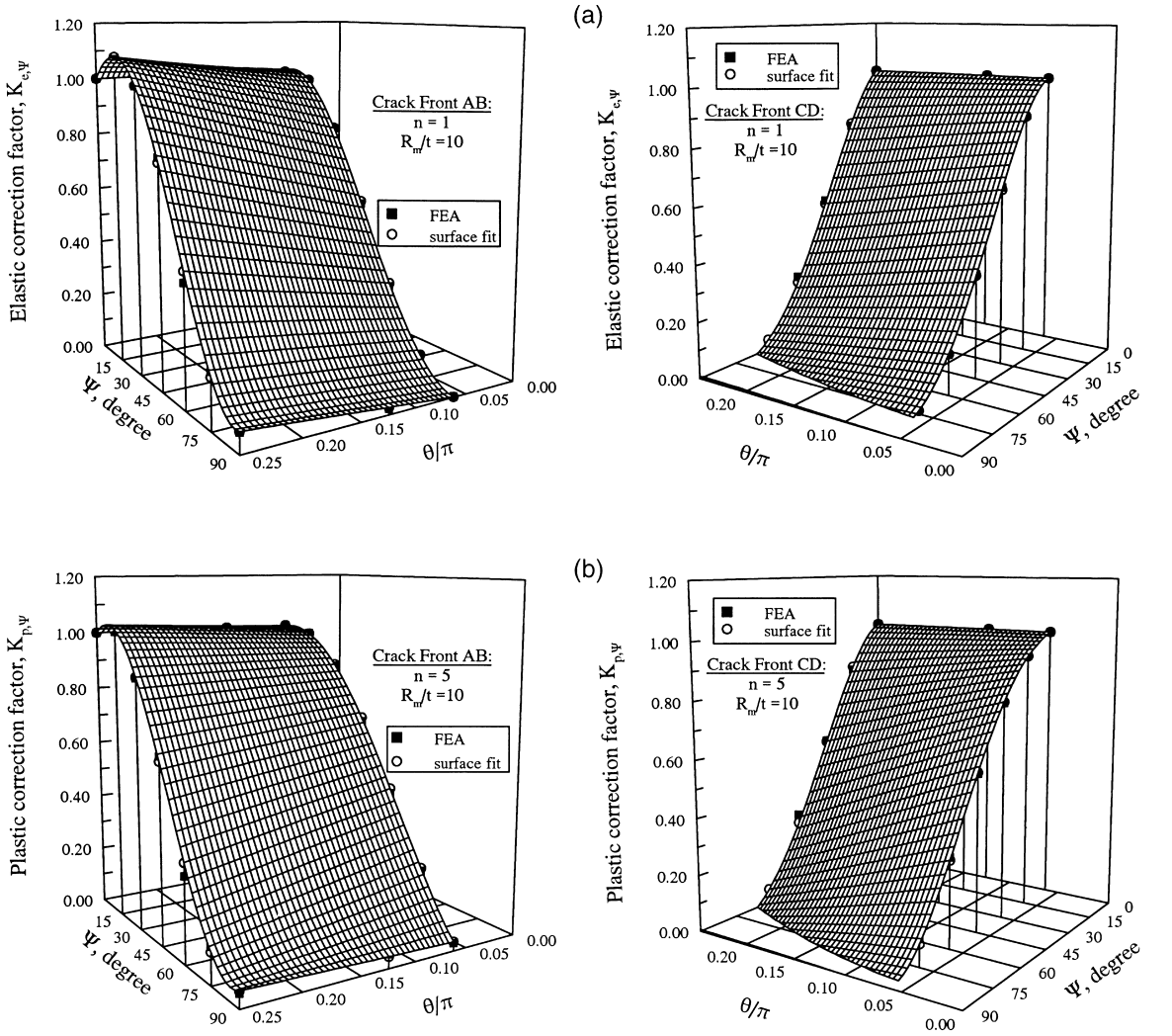

Fig. 14. Elastic and plastic correction factors for $R_m/t = 10$: (a) elastic correction factors for crack fronts AB and CD ($n = 1$) and (b) plastic correction factors for crack fronts AB and CD ($n = 5$).

it is in an area of extrapolation. It is also recommended that the surface fit equations for crack front CD be used only for crack lengths between 1/16 and 1/4 of the circumference.

6. Summary and conclusions

New elastic and elastic–plastic finite element solutions of J-integral are presented for off-center, TWCs in pipes under pure bending. The analyses involved a three-dimensional nonlinear FEM and small-strain theory. Using the ABAQUS commercial code, 105 analyses were performed for a pipe with a radius-to-thickness ratio of 10 and a wide variety of crack sizes, off-center angles, and material hardening exponents. The results show that:

- The J-integrals of pipes with symmetrically centered TWCs, calculated by the present three-dimensional FEA, compare very well with the existing GE/EPRI solutions.
- For TWCs in pipes, the J-integral for an off-center crack is smaller than that for a symmetrically centered crack for most offset angles. This implies that the load-carrying capacity of a pipe containing an off-center crack can be higher than that of a pipe containing a symmetrically centered crack.
- A threshold of off-center angle exists below which the J values of an off-center crack at the crack front farther away from the bending axis of the pipe may exceed those of a symmetrically centered crack. The threshold off-center angles found in this study were small, as was their effect on the J values.
- The J-integrals at the two crack fronts of an off-center crack are unequal due to the loss of symmetry with respect to the bending plane of the pipe. In general, the J-integral is larger, and hence, critical at the crack front which is farther away from the bending axis of the pipe. This is because, at that crack front, the tensile stress is larger and the component of applied moment about the crack centerline has a further crack-opening effect.

Finally, the FEM solutions generated in this study were used to develop new analytical expressions of influence functions and J-integral for fracture analysis of pipes containing off-center cracks. This would significantly reduce the computational effort in performing any future probabilistic and crack-growth studies.

Acknowledgements

The work presented in this paper was supported by the Faculty Early Career Development Program of the U.S. National Science Foundation (Grant No. CMS-9733058). The program directors were Dr. Sunil Saigal and Dr. Ken Chong.

Appendix A. Influence functions for symmetric cracks

In Eq. (8), $F(\theta/\pi, R_m/t)$ is a dimensionless elastic influence function that depends on pipe and crack geometry. According to Rahman [38],

$$F(\theta/\pi, R_m/t) = 1 + \{ A_1 \quad A_2 \quad A_3 \} \begin{Bmatrix} (\theta/\pi)^{1.5} \\ (\theta/\pi)^{2.5} \\ (\theta/\pi)^{3.5} \end{Bmatrix} \{ B_1 \quad B_2 \quad B_3 \quad B_4 \} \begin{Bmatrix} 1 \\ (R_m/t) \\ (R_m/t)^2 \\ (R_m/t)^3 \end{Bmatrix} \tag{14}$$

where A_i (i = 1–3) and B_i (i = 1–4) are constant coefficients. Let $\boldsymbol{A} = \{ A_1 \quad A_2 \quad A_3 \}^T$ and $\boldsymbol{B} = \{ B_1 \quad B_2 \quad B_3 \quad B_4 \}^T$ be two real vectors with the coefficients, A_i and B_i as their components, respectively. Using best fit of finite element results, $\boldsymbol{A}$ and $\boldsymbol{B}$ are given by [38]:

$$\boldsymbol{A} = \{ 0.006215 \quad 0.013304 \quad -0.01838 \}^T \tag{15}$$

$$\boldsymbol{B} = \{ 175.577 \quad 91.69105 \quad -5.53806 \quad 0.15116 \}^T. \tag{16}$$

In Eq. (9), $h_1(\theta/\pi, n, R_m/t)$ is a dimensionless plastic influence function that depends on pipe geometry, crack geometry, and material hardening exponent. According to Rahman [38],

$$h_1(\theta/\pi, n, R_m/t) = \{\, 1 \quad (\theta/\pi) \quad (\theta/\pi)^2 \quad (\theta/\pi)^3 \,\} \begin{bmatrix} C_{00} & C_{10} & C_{20} & C_{30} \\ C_{01} & C_{11} & C_{21} & C_{31} \\ C_{02} & C_{12} & C_{22} & C_{32} \\ C_{03} & C_{13} & C_{23} & C_{33} \end{bmatrix} \begin{Bmatrix} 1 \\ n \\ n^2 \\ n^3 \end{Bmatrix} \tag{17}$$

where C_{ij} $(i, j = 0\text{–}3)$ are coefficients which depend on R_m/t and can also be calculated from best fit of finite element results [38]. Let $\boldsymbol{C} = [C_{ij}]$, i, $j = 0\text{–}3$, be a real matrix with the coefficients, C_{ij} as its components. According to Rahman [38], $\boldsymbol{C}$ is given by:

For $R_m/t = 5$,

$$\boldsymbol{C} = \begin{bmatrix} 3.74009 & 1.43304 & -0.10216 & 0.0023 \\ -0.19759 & -10.19727 & -0.45312 & 0.04989 \\ 36.42507 & 17.03413 & 3.36981 & -0.21056 \\ -70.4846 & -14.69269 & -2.90231 & 0.15165 \end{bmatrix} \tag{18}$$

For $R_m/t = 10$,

$$\boldsymbol{C} = \begin{bmatrix} 3.39797 & 1.31474 & -0.07898 & 0.00287 \\ -3.07265 & 4.34242 & -2.48397 & 0.11476 \\ 131.7381 & -79.02833 & 16.18829 & -0.66912 \\ -234.6221 & 117.0509 & -20.30173 & 0.79506 \end{bmatrix} \tag{19}$$

For $R_m/t = 20$,

$$\boldsymbol{C} = \begin{bmatrix} 4.07828 & -1.55095 & 0.67206 & -0.0442 \\ -18.21195 & 69.92277 & -18.41884 & 1.11308 \\ 357.4929 & -453.1582 & 108.0204 & -6.56651 \\ -602.7576 & 617.9074 & -144.9435 & 8.9022 \end{bmatrix}. \tag{20}$$

See Ref. [38] for further explanations on how these coefficients were calculated.

Appendix B. Coefficients D_{ij}

Let $\boldsymbol{D} = [D_{ij}]$, $i = 0, 1, \ldots, 7$ and $j = 0, 1, \ldots, 4$, be a real matrix with the coefficients, D_{ij}, as its components. Following least-squares curve-fit, $\boldsymbol{D}$ for $R_m/t = 10$ is given by:

At crack front AB,

$$\boldsymbol{D} = \begin{bmatrix} 0.3528 & -0.2522 & 0.0631 & -0.0074 & 0.0003 \\ 2.7962 & -1.0617 & 0.2940 & -0.0266 & 0.0008 \\ -2.9981 & 1.6897 & -0.4233 & 0.0496 & -0.0021 \\ 3.7670 & -2.0229 & 0.3196 & -0.0762 & 0.0047 \\ 2.0620 & -1.4627 & 0.3823 & -0.0467 & 0.0020 \\ -7.1406 & 2.5393 & -0.5405 & 0.1119 & -0.0064 \\ -0.3596 & 0.3150 & -0.0885 & 0.0115 & -0.0005 \\ 2.3539 & -0.5121 & 0.1318 & -0.0327 & 0.0019 \end{bmatrix} \tag{21}$$

At crack front CD,

$$\boldsymbol{D} = \begin{bmatrix} 0.1444 & -0.2620 & 0.0651 & -0.0064 & 0.0002 \\ -3.1782 & 2.5246 & -0.6779 & 0.0734 & -0.0029 \\ -3.3451 & 2.3779 & -0.5637 & 0.0583 & -0.0022 \\ 4.2744 & -8.1376 & 1.9887 & -0.2243 & 0.0094 \\ 2.9435 & -2.6898 & 0.6399 & -0.0670 & 0.0026 \\ -0.6972 & 6.2504 & -1.4695 & 0.1750 & -0.0077 \\ -0.7191 & 0.8152 & -0.1955 & 0.0207 & -0.0008 \\ -0.4701 & -1.3246 & 0.3025 & -0.0393 & 0.0019 \end{bmatrix}. \tag{22}$$

References

[1] USNRC. Report to the U.S. Nuclear Regulatory Commission Piping Review Committee. Prepared by Pipe Break Task Group, NUREG/CR-1061, vol. 3. Washington, DC: U.S. Nuclear Regulatory Commission, November 1984.

[2] Federal Register. Standard Review Plan, Section 3.6.3 Leak-Before-Break Evaluation Procedures. Public comment paper, vol. 52, No. 167. Notices, August 1987. pp. 32626–633.

[3] American Society of Mechanical Engineers, ASME. Boiler and Pressure Vessel Code, Section XI, 1989.

[4] Rahman S, Brust F, Ghadiali N, Choi YH, Krishnaswamy P, Moberg F, Brickstad B, Wilkowski G. Refinement and evaluation of crack-opening-area analyses for circumferential through-wall cracks in pipes. NUREG/CR-6300. Washington, DC: U.S. Nuclear Regulatory Commission, April 1995.

[5] Rahman S, Ghadiali N, Wilkowski G, Bonora N. Effects of off-centered crack and restraint of induced bending on the crack-opening-area analysis of pipes. In: Mehta H, editor. Proceedings of 1995 ASME/JSME Pressure Vessels and Piping Conference, Honolulu, Hawaii, Fatigue and Fracture Mechanics in Pressure Vessels and Piping, PVP-Vol. 304, 1995. p. 149–62.

[6] Rahman S, Ghadiali N, Wilkowski G, Bonora N. Effects of off-centered crack and restraint of induced bending due to pressure on the crack-opening-area analysis of pipes. Nuclear Engineering and Design 1997;167:55–67.

[7] Wilkowski GM, et al. Short cracks in piping and piping program. NUREG/CR-4599, vols. 1–3, Nos. 1–2. Washington, DC: U.S. Nuclear Regulatory Commission, 1991–1994.

[8] Brust FW, Scott P, Rahman S, Ghadiali N, Kilinski T, Francini B, Marschall CW, Miura N, Krishnaswamy P, Wilkowski GM. Assessment of short through-wall circumferential cracks in pipes — experiments and analysis. NUREG/CR-6235. Washington, DC: U.S. Nuclear Regulatory Commission, April 1995.

[9] Ghadiali N, Rahman S, Choi YH, Wilkowski G. Deterministic and probabilistic evaluations for uncertainty in pipe fracture parameters in leak-before-break and in-service flaw evaluations. Topical Report, NUREG/CR-6443. Washington, DC: U.S. Nuclear Regulatory Commission, June 1996.

[10] Rahman S, Brust FW, Ghadiali N, Wilkowski G. Crack-opening-area analyses for circumferential through-wall cracks in pipes. Part I: Analytical models. International Journal of Pressure Vessels and Piping 1998;75(5):357–73.

[11] Rahman S, Brust FW, Ghadiali N, Wilkowski G. Crack-opening-area analyses for circumferential through-wall cracks in pipes. Part II: Model validations. International Journal of Pressure Vessels and Piping 1998;75(5):375–96.

[12] Rahman S, Brust FW, Ghadiali N, Wilkowski G. Crack-opening-area analyses for circumferential through-wall cracks in pipes. Part III: Off-center cracks, restraint of bending, thickness transition, and weld residual stresses. International Journal of Pressure Vessels and Piping 1998;75(5):397–415.
[13] Rice JR. A path independent integral and the approximate analysis of strain concentration by notches and cracks. Journal of Applied Mechanics 1968;35:379–86.
[14] Hutchinson JW. Singular behavior at the end of a tensile crack in a hardening material. Journal Mech Phys Solids 1968;16:13–31.
[15] Rice JR, Rosengren GF. Plane strain deformations near a crack tip in a power-law hardening material. Journal Mech Phys Solids 1968;16:1–12.
[16] Shih CF, Moran B, Nakamura T. Energy release rate along a three-dimensional crack front in a thermally stressed body. International Journal of Fracture 1986;30:79–102.
[17] Moran B, Shih CF. A general treatment of crack tip contour integrals. International Journal of Fracture 1987;35:295–310.
[18] Anderson TL. Fracture mechanics: fundamentals and applications, 2nd ed. Boca Raton, FL: CRC Press, 1995.
[19] ABAQUS, User's Guide and Theoretical Manual, Version 5.6. Hibbitt, Karlsson, and Sorensen, Pawtucket, RI, 1997.
[20] MSC/PATRAN, User's Guide and Theoretical Manual, Version 7. The MacNeal–Schwendler Corporation, Los Angeles, CA, 1997.
[21] Wilkowski GM, et al. Degraded piping program — phase II, final and semiannual reports. NUREG/CR-4082, vols. 1–8. Washington, DC: U.S. Nuclear Regulatory Commission, 1985–1989.
[22] Schmidt RA, Wilkowski G, Mayfield M. The international piping integrity research group (IPIRG) program — an overview. Proceedings of 11th International Conference on Structural Mechanics in Reactor Technology, Paper G23/1, August 1991.
[23] Hopper A, Mayfield M, Olson R, Scott P, Wilkowski G. Overview of the IPIRG-2 program — seismic loaded cracked pipe system experiments. Proceedings of 13th International Conference on Structural Mechanics in Reactor Technology, Division F, Paper F12-1, August 1995.
[24] Rahman S, Olson R, Rosenfield A, Wilkowski G. Summary of results from the IPIRG-2 Round-Robin analyses. NUREG/CR-6337. Washington, DC: U.S. Nuclear Regulatory Commission, February 1996.
[25] Krishnaswamy P, Scott P, Choi Y, Mohan R, Rahman S, Brust F, Wilkowski G. Fracture behavior of short circumferentially surface-cracked pipe. Topical Report, NUREG/CR-6298. Washington, DC: U.S. Nuclear Regulatory Commission, November 1995.
[26] Scott P, Francini R, Rahman S, Rosenfield A, Wilkowski G. Fracture evaluations of fusion line cracks in nuclear pipe bimetallic welds. Topical Report, NUREG/CR-6297. Washington, DC: U.S. Nuclear Regulatory Commission, April 1995.
[27] Rahman S, Brust F. An estimation method for evaluating energy release rates of circumferential through-wall cracked pipe welds. Engineering Fracture Mechanics 1992;43(3):417–30.
[28] Rahman S, Brust F. Elastic–plastic fracture of circumferential through-wall cracked pipe welds subject to bending. Journal of Pressure Vessel Technology 1992;114(4):410–6.
[29] Rahman S, Wilkowski G, Brust F. Fracture analysis of full-scale pipe experiments on stainless steel flux welds. Nuclear Engineering and Design 1996;160:77–96.
[30] Kumar V, German MD, Wilkening WW, Andrews WR, deLorenzi HG, Mowbray DF. Advances in elastic–plastic fracture analysis. EPRI NP-3607. Palo Alto, CA: Electric Power Research Institute, 1984.
[31] Kumar V, German M. Elastic–plastic fracture analysis of through-wall and surface flaws in cylinders. EPRI Topical Report, NP-5596. Palo Alto, CA: Electric Power Research Institute, January 1988.
[32] Brust F, Rahman S, Ghadiali N. Elastic–plastic analysis of small cracks in tubes. Journal of Offshore Mechanics and Arctic Engineering 1995;117(1).
[33] Brust F, Rahman S, Ghadiali N. Elastic–plastic analysis of small cracks in tubes. In: Proceedings of 11th International Conference of Offshore Mechanics and Arctic Engineering, Calgary, Canada, June. 1992.
[34] ADINA, User's Guide and Theoretical Manual. Report AE81-1, ADINA Engineering, Watertown, MA, 1984.
[35] Firmature R. Elastic–plastic analysis of off-centered cracks in cylindrical structures. A Thesis for Master of Science, The University of Iowa, Iowa City, IA: Department of Mechanical Engineering, July 1998.
[36] Rahman S, Firmature R. Elastic–plastic analysis of off-centered cracks in cylindrical structures. In: Rahman S, editor. Proceedings of 1998 ASME/JSME Pressure Vessels and Piping Conference, San Diego, CA, Fatigue, Fracture and Residual Stresses, PVP-Vol. 373. July 1998. pp. 489–509.
[37] Rahman S, Chen G, Firmature R. Probabilistic elastic–plastic analysis of off-centered cracks in cylindrical structures. In: Rahman S, editor. Proceedings of 1999 ASME Pressure Vessels and Piping Conference, Boston, MA, Probabilistic and Environmental Aspects of Fracture and Fatigue, PVP-Vol. 390. August 1999.
[38] Rahman S. A stochastic model for elastic–plastic fracture analysis of circumferential through-wall-cracked pipes subject to bending. Engineering Fracture Mechanics 1995;52(2).